Ecological Engineering xxx (2016) xxx–xxx

Contents lists available at ScienceDirect

Ecological Engineering

journal homepage: www.elsevier.com/locate/ecoleng

Recovering hydromorphological functionality to improve natural purification capacity of a highly human-modified wetland

J.M. Bodoque[a,*], J. Ladera[a], J.L. Yela[b], J. Alonso-Azcárate[c], D. Brito[d], I. Antigüedad[e], R. Duran[f], E. Attard[f], B. Lauga[f], J.M. Sánchez-Pérez[g]

[a] Department of Geological and Mining Engineering, University of Castilla La Mancha, Toledo, Spain
[b] DITEG Research Group, Faculty of Environmental Sciences and Biochemistry, University of Castilla-La Mancha, Toledo, Spain
[c] Department of Physical Chemistry, Faculty of Environmental Sciences and Biochemistry, University of Castilla-La Mancha, Avenida Carlos III, s/n, 45071 Toledo, Spain
[d] MARETEC, Instituto Superior Técnico, Universidade de Lisboa, Lisbon, Portugal
[e] Department of Geodynamics, University of the Basque Country (UPV/EHU), P.O. Box 644, E-48080 Bilbao, Basque Country, Spain
[f] Equipe Environnement et Microbiologie, Université de Pau et des Pays de l'Adour, IPREM UMR CNRS 5254, BP 1155, 64013 Pau Cedex, France
[g] ECOLAB, Université de Toulouse, CNRS, INPT, UPS, Toulouse, France

ARTICLE INFO

Article history:
Received 14 May 2015
Received in revised form 11 February 2016
Accepted 12 February 2016
Available online xxx

Keywords:
Denitrification
Flood pulses
Hydromorphology
Agricultural floodplain
Irrigation

ABSTRACT

Modification of the hydrological regime by human actions can reduce the capacity of wetlands to improve water quality. For the first time, a study was conducted of the inherent pollution attenuation capacity of wetlands associated with the highly regulated Spanish Tagus River. We determined the natural purification capacity of a floodplain where irrigated agriculture predominates and hydraulic connection with the river is virtually nonexistent. To this end, continuous hydrophysical measurements and sediment and water samples were taken during the period extending from April 2013 to March 2014. A multiparametric dataset including hydraulic, physico-chemical, bacterial and macroinvertebrate indicators was collected from ten piezometers located within a meander, together with two additional sampling points in the river. Sampling was performed monthly to measure hydraulic and physico-chemical parameters and quarterly for bacteria and macroinvertebrates. The data enabled us to implement different but complementary methodological approaches to characterize denitrification. Specifically, we performed: (i) end-member mixing analysis (EMMA); (ii) macroinvertebrate characterization; (iii) denitrification potential analysis; (iv) bacterial assemblage structure analysis; and (v) hydrological modeling of the current and different future management scenarios. All the approaches except EMMA indicated the same conclusion: denitrification is almost nonexistent due to the fact that the study site does not present the hydric soil and oxygen-limited conditions required to enable denitrification. The EMMA analysis showed that theoretical nitrate concentrations were lower than expected in some areas during the summer months (e.g. $\Delta NO_3 = -41$ in August 2013), which may have been because irrigation intensity was spatio-temporal variable at the study site. Our results show that floodplain denitrification has been drastically reduced due to the suppression of flood pulses. In this context, restoration of the hydrological regime in riverine wetlands would lead to the decay of nitrates whose dynamic evolution increases with flooding, as scenarios tested by the MOHID hydro-biogeochemical model have demonstrated.

1. Introduction

It is well-known that when wetlands are in a good state of conservation and the associated river is hydromorphologically functional, they are biogeochemically active as regards their capacity to mitigate pollution (Pinay et al., 2002; Sánchez-Pérez and Trémolières, 2003; Iribar et al., 2008). An example of the above is denitrification. This natural attenuation process requires oxygen-limited conditions and organic matter that are often associated with the hydric soil characteristics of most natural wetlands (Sánchez-Pérez et al., 2003a; Hernandez and Mitsch, 2007; Song et al., 2014).

The concept of hydromorphology was introduced by the EU Water Framework Directive (WFD; European Commission, 2000).

* Corresponding author.
E-mail address: josemaria.bodoque@uclm.es (J.M. Bodoque).

http://dx.doi.org/10.1016/j.ecoleng.2016.02.013
0925-8574/© 2016 Elsevier B.V. All rights reserved.

It takes into account modifications that occur in flow regimes and, as a result, in the efficiency with which fluvial processes are able to have an impact on the geomorphology of rivers. In this regard, the pollution control explained in the previous paragraph is a direct consequence of the hydrological regime of rivers (Middleton, 2002), since it requires the existence of alternate floods and flows below bankfull discharge. The transport of particulate and dissolved compounds and carbon supply is facilitated during floods and this will provide energy to the bacteria directly responsible for the biogeochemical reactions to transform nitrate to nitrogen gas through denitrification (Hernandez and Mitsch, 2006). The environmental factor that facilitates this combination of environmental conditions and bacteria activity is the adequate hydric status of soil (Rabot et al., 2014).

Suitable soil wetness is achieved by both good hydraulic connectivity between the river and the alluvial aquifer and a seasonal high water table. In addition, vegetation existing in wetlands provides easily degradable organic compounds that macro and microinvertebrates can take advantage of and supply high energy carbon for bacterial activity (Mermillod-Blondin et al., 2003).

The modification of the hydrological regime, due to the existence of reservoirs and inter-basin water transfer systems, may cause the absence of hydraulic connectivity between the river and the alluvial aquifer (Kingsford, 2000). As a consequence, groundwater flows through the floodplain are altered and this reduces the capacity of wetlands to improve water quality (Hunt et al., 2014). The above may occur if the frequency of ordinary floods is increased, which will affect the trophic web through leaf production by tree-breakdown, fragmentation and decomposition by macro and microinvertebrates and nutrient assimilation (and pollutant degradation) by bacteria (Kjellin et al., 2007). In addition, pollution control is affected if the intensity and duration of floods are not sufficient to maintain and develop “hot spots” and “hot moments” in the floodplain (Groffman et al., 2009).

This paper aims to assess the natural purification capacity of a wetland linked to a highly human-modified river, in which ordinary floods do not occur and where the alluvial aquifer is mainly recharged by irrigation. In this context, it is also intended to test management scenarios, through the use of the MOHID hydro-biogeochemical model, that help to enhance pollution control in wetlands that have been highly altered by very significant modifications in their hydrological regime.

2. Material and methods

2.1. Study site description

The study site is situated in a meander of the Tagus River, roughly in the middle of the Iberian Peninsula (Fig. 1). The climate is continental Mediterranean, with a mean annual rainfall and temperature of 375 mm and 15 °C, respectively. The drainage area of the Tagus watershed at the study site covers about 27,600 km^2. A reservoir located 9 km upstream feeds water into an 18 km long irrigation channel (see Fig. 1). Over the past 13 years, the estimated annual average flow has been 5.47 $m^3\,s^{-1}$. On average, September is the month with the lowest flow (i.e. 4.33 $m^3\,s^{-1}$), while the highest flows have been measured in October (i.e. 9.40 $m^3\,s^{-1}$ on average). The daily flow within the period for which records are available ranged from 1.06 $m^3\,s^{-1}$ to 101.10 $m^3\,s^{-1}$ (http://sig.magrama.es/aforos/).

The land use is predominantly agricultural, except for a narrow strip along the inside edge of the meander, which is occupied by a pasture and where the presence of riparian forest is marginal. The remaining surface is dedicated to alternative crops of irrigated cereal (i.e. corn, barley, wheat) and vegetables (i.e. tomatoes). The whole area is fertilized using pig manure and chemical fertilizers. In addition, different kinds of herbicides (i.e. terbutylazine and metolachlor) are used to kill unwanted plants.

Hydraulic conductivity is 10^{-4} m/s and the alluvial aquifer is not hydraulically controlled by river levels. In its stead, water table is mostly influenced by water coming from the Castrejón irrigation channel, which is located about 2 km north of the study site. The irrigation period usually begins in May and ends in late September. As main irrigation systems, is worth to note: flooding; sprinkler and drip. The water table ranges from 1 m (near river banks), and 5 m inside the meander.

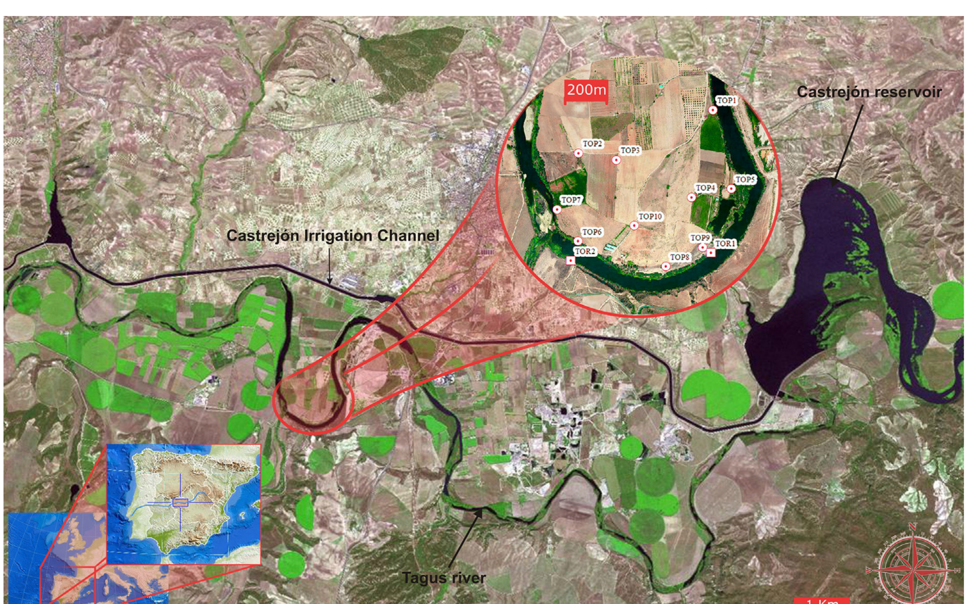

Fig. 1. Location of the study site. The notation “TOP” indicates how piezometers are spatially distributed in the meander studied.

2.2. Methodological approach implemented

Different methodologies have been put into practice and, while there is no hierarchical dependency between them, they do complement each other. This approach helps to better characterize the self-purification capability of a highly modified wetland. Specifically, the following methodological stages were addressed: (i) hydrological and hydrochemical characterization of the wetland system; (ii) end-member mixing analysis (EMMA); (iii) characterization of the macroinvertebrates present in groundwater; (iv) analysis of the denitrification enzymatic activity; (v) analysis of the denitrifier communities and their abundance using a molecular approach; and (vi) implementation of the MOHID hydro-biogeochemical model.

2.2.1. Hydrological and hydrochemical characterization

Ten piezometers were installed at locations that would help characterize both general and local flow patterns, (i.e. areas of hydraulic connectivity between the river and the alluvial aquifer). A differential GPS with centimetric accuracy was used to measure the hydraulic heads with respect to the national datum level. CDT DIVER data loggers (Schlumberger Water Services) were used to carry out continuous hydrophysical measurements during the period extending from April 2013 to March 2014. Specifically, CTD DIVERS were installed in 3 piezometers in locations that enabled the piezometric dynamic to be properly controlled. A fourth was situated in the river in order to monitor variations of water depths and, consequently, the existence of hydraulic connectivity between the river and the alluvial aquifer. A baro-diver was also installed to correct hydraulic heads, in case of sudden changes in atmospheric pressure. The parameters recorded were: (i) water depth; (ii) water temperature and (iii) the electrical conductivity of water at 10-min intervals.

Physical-chemical measurements and samples were collected every month and after pumping long enough in order to guarantee that the water sampled had characteristics corresponding to the alluvial aquifer. Dissolved oxygen, temperature, pH, redox potential and electrical conductivity were measured in the field with a multiprobe YSI sonde (YSI Incorporated, Yellow Springs, Ohio) attached to a handheld data logger (YSI Sonde Model 6820 WITH 650 MDS), while a sonde was used to measure water depth. With regard to dissolved organic carbon (DOC), water samples collected were filtered using precombusted GFF filters and analyzed using a platinum catalyzer at 680 °C (Shimadzu TOC-VCSH analyzer). Lastly, nitrates were determined with the spectrophotometer Lovibond SpectroDirect.

2.2.2. End-member mixing analysis and variations rates of nitrates

An end-member mixing analysis, EMMA (Christophersen et al., 1990) using conservative components was conducted to calculate the proportion of water from two sources. In the case we studied, the selected poles or end members comprised surface water from irrigation, which is characterized by a lower nitrate concentration and electrical conductivity (1–44 mg/L; 955–2700 $\mu S\,cm^{-1}$), and groundwater highly affected by agricultural management practices, which presents a higher nitrate concentration and electrical conductivity (11–120 mg/L; 2193–3405 $\mu S\,cm^{-1}$).

Taking the results obtained from the EMMA into account, the theoretical concentration of NO_3 and DOC for each control point was calculated using the following equation:

$$[CT]i = (\%CH * [C]CH) + (\%P * [C]P) \tag{1}$$

where $[CT]i$ is the theoretical concentration of NO_3 or DOC, % is the percentage of water from each end member, and the subscripts *CH* (water coming from irrigation) and *P* (groundwater affected by agricultural practices) are the control points considered and each of the end-members, respectively.

Once the theoretical concentrations of NO_3 or DOC were calculated, they were compared with the real concentrations, thereby obtaining the rates of variation (depletion or enrichment) of nitrates.

$$\Delta C = \frac{[CR]i - [CT]i}{[CT]i} \tag{2}$$

In the places where ΔC was negative there was consumption/depletion of these compounds, meaning that attenuation processes might be taking place at these points. In contrast, in the places where ΔC was positive there was an enrichment/increase, so a point-source input might be contributing to higher concentrations of NO_3. Geochemical maps of the distribution of the differences between expected and measured concentrations were made for each month of the sampling period. For this purpose, spline analysis of interpolation was performed using ArcGIS 10.1.

2.2.3. Taxonomic and functional composition of groundwater macroinvertebrates

A groundwater invertebrate sample was collected at each piezometer every 3 months for 1 year: (April 2013, July 2013, October 2013 and February 2014). Invertebrate communities were sampled by pumping water using the Bou-Rouch method (Boulton et al., 2008) with a hand pump. For the river sampling sites, a Bou-Rouch pipe, a metal pipe with nine rows of 5-mm-diameter holes at 4 cm from the distal end of the pipe, was inserted around 20 cm into the sediment. At each sampling point (piezometers and river) 90–100 L of groundwater was pumped into a bucket through two successive plankton nets with mesh sizes of 250 μm and 50 μm for macrofauna and meiofauna collection, respectively. Samples were preserved in situ in 70% ethanol at 5 °C.

Invertebrate samples were sorted and identified in the laboratory to at least order level using a binocular microscope (at $\times$10–40 magnification). Feeding habits, biogeochemical filtration capacity, and the particulate organic matter (POM) breakdown capacity were used to characterize the functional composition of the macroinvertebrate assemblage. Affinity (0–5) scores were used for each of the following feeding behaviors: scraper; deposit feeder; shredder; scraper; filter-feeder; piercer; predator and parasite (following Tachet et al., 2010). A score of zero indicates no affinity, while a score of 5 indicates the highest affinity of the taxon to a particular feeding habit. For taxa identified at higher taxonomic levels than genera, the most frequent score across all taxa belonging to a particular taxonomic group was selected. The SITES $\times$ TAXA abundance matrix was multiplied by the TAXA $\times$ FEEDING HABITS matrix to calculate three functional diversity metrics: abundance of individuals showing affinity for each feeding habitat (i.e. functional abundance), total richness of feeding habits (i.e. functional richness), and the Shannon–Wiener diversity of feeding habits (i.e. functional Shannon's diversity index). To assess the biogeochemical filtration and POM breakdown capacities of the assemblage, we used the functional scores defined by Boulton et al. (2008). Thus for each taxa, a biogeochemical filtration and POM breakdown efficiency score was assigned: 0, no or unknown direct role; 1, minor role; 2, moderate role; and 3, major role. We expressed the biogeochemical filtration capacity of the groundwater assemblage as the product of the absolute abundance of each taxa and its efficiency score.

2.2.4. Denitrification potential

The potential rate of the denitrification phase was quantified using the denitrification enzyme activity (DEA) assay with the acetylene block technique (Smith and Tiedje, 1979). In the first stage, moist soil samples from the field corresponding to each piezometer were homogenized after collection and kept refrigerated at 4 °C until DEA assay. Next, three replicate assays were performed per sample in 150 mL Erlenmeyer flasks. In order to guarantee that the incubation environment was always the same, Milli-Q water, with added KNO_3 and $C_2H_3NaO_2$, was used until final concentrations of 100 mg N/L and 50 mg C/L, respectively, were reached. The anaerobic state of incubation flasks was achieved by bubbling with N_2 gas for 11 min (including 1 min headspace flush) and subsequently verifying complete deoxygenation with an oxygen-sensing probe. Next, 15 mL of acetylene (C_2H_2) was added and in order to ensure equal distribution of acetylene and N_2O, the flasks were shaken on a rotary shaker. 5 mL of gas was sampled at 5 min, 2 h, 4 h and 6 h after injection of C_2H_2. The resulting gas samples were stored in 10-mL evacuated collection tubes (Venoject; Terumo Europe N.V., Leuven, Belgium) and were subsequently analyzed for N_2O concentrations using an ECD varian CP 3800 gas chromatography fitted with an electron capture detector.

2.2.5. Bacterial assemblage structure

During the sampling period (i.e. April 2013 to March 2014), sediment was collected quarterly by pumping from the piezometers and kept at −80 °C until DNA extraction. Before DNA extraction the water phase was removed by centrifugation at 3000 rpm for 5 min. Metagenomic DNA from sediments was extracted with the power Soil DNA kit (MoBio Laboratories Ozyme, St Quentin en Yvelines, France) following the manufacturer's recommendations. DNA was eluted in 50 μL water and stored at −20 °C until use.

The bacterial 16S rRNA genes were amplified using the universal primers 357F (5′-CCTACGGGAGGCAGCAG-3′) (Teske et al., 1996) and 926R (5′-CCGTCAATTCMTTTRAGT-3′) (Lane, 1991). Forward primer was 5′ labeled with carboxyfluorescein (FAM). The PCR conditions were initial denaturation (98 °C for 30 s) followed by 30 cycles of denaturation (98 °C for 10 s), annealing (58 °C for 30 s), and extension (72 °C for 30 s) and a terminal extension at 72 °C for 10 min. The reaction mixture contained 200 mM of dNTP, 0.5 μM of each primer, 0.25 μL of the Q5 High-Fidelity Taq polymerase (New England Biolabs Evry, France), 2.5 μL of 10× buffer and 1 μL of DNA template. Sterile distilled water was added to obtain a final volume of 25 μL. PCR products were checked by agarose gel electrophoresis and purified with the PCR purification kit (GE Healthcare Velizy-Villacoublay, France). The purified 16S rRNA amplified fragments (100 ng per sample) were digested by 3 U of AluI restriction enzyme (New England Biolabs Evry, France) at 37 °C in a final volume of 10 μL for 3 h. The digested products (1 μL) were mixed with 8.75 μL of deionized formamide and 0.25 μL of the Genescan ROX 500 size standard (Applied Biosystems). Fluorescently labeled fragments were separated and detected with ABI PRISM 3130xl Genetic Analyzer (Applied Biosystems). Data were processed using GENEMAPPER software (version 1.4, Applied Biosystems) to produce raw T-RFLP profiles. These profiles were normalized and analyzed using the online software T-REX (Culman et al., 2009) to produce the final T-RF data matrix. Only terminal fragments whose size ranged from 35 bp to 500 bp and whose height was greater than 30 fluorescence units were considered for analysis (Volant et al., 2014). Shannon and Evenness indexes were calculated from T-RFLP patterns using the MVSP software (Multi-Variate Statistical Package 3.12d, Kovach Computing Services, 1985–2001, UK).

2.2.6. Hydrological modeling

The numerical model used was MOHID Land (Trancoso et al., 2009). Transport of dissolved organic carbon and nitrate was simulated using a simple model for organic matter decay (i.e. dissolved organic carbon and particulate organic carbon, POC) and denitrification adapted from Peyrard et al. (2011). The model was implemented using LiDAR data with 1 m resolution, and local soil and land use info. The model is compared with field data (i.e. piezometer levels and concentrations).

The Tagus site has irrigated fields in almost all areas; as no data were available, irrigation was estimated from piezometer level rise. The aquifer level rise in the upper part is around 5 mm/day (i.e. accounting for porosity). The reference evapotranspiration is around 2–3 mm/day so irrigation should be around 8 mm/day to compensate. A constant irrigation in the model of 8 mm/day was introduced for 1 month (i.e. July, the month when the level rises) and the reference evapotranspiration was constant at 2.4 mm/day. The aquifer level in the boundary was set as 400 m; that is, the usual average aquifer and river surface height, since Tagus level changes are very limited (less than 0.5 m during the period studied). Initial aquifer nitrate and DOC concentration were obtained from the interpolated concentrations from the piezometer values at the beginning of the simulation. The model was run based on a daily time-step for the period May to September 2013, when for the field data period piezometer level changes occurred due to irrigation. The model was used to depict the changes associated with management scenarios based on changing boundary conditions. Specifically, the scenarios considered were: (i) 100% increase in DOC in the river; (ii) 50% decrease in DOC in the river; (iii) 100% increase in NO_3 concentration in the aquifer; (iv) 50% decrease in nitrate concentration in the aquifer; and (v) 50% increase in river discharge. An additional scenario was simulated by forcing the occurrence of floods.

2.2.7. Statistical analysis

Statistical analysis was performed with SPSS version 19 for Windows. Kolmogorov–Smirnov and Shapiro–Wilk's tests were used to check the normality of physical-chemical parameters, DOC, nitrates and rates of denitrification potential. Non-parametric techniques were chosen, since all variables considered, except electrical conductivity, did not define populations that fit normal distribution, even after normalization. Specifically, the statistical dependence existing between denitrification potential and the other variables considered is analyzed by using the Spearman's rank correlation coefficient or Spearman's rho. In addition, as far as denitrification rates are concerned, we looked at whether there were statistically significant differences between the various campaigns, as well as between piezometers. For this purpose, the Kruskal–Wallis one-way analysis of variance by ranks, which is a non-parametric method for testing whether samples originate from the same distribution, was used. This analysis is designed to demonstrate the extent to which irrigation is an activating factor of the denitrification process.

Statistical data based on the characterization of invertebrates was analyzed in order to determine the relationship between the diversity indices used in the study and fluvial dynamics. For this purpose, the Kruskal–Wallis non-parametric text was applied as the data in the diversity indices did not fit the normal distribution, again even after normalization. In this regard, we looked for statistically significant differences between: (i) the sampling campaigns; (ii) the piezometers; and (iii) the piezometers depending on their proximity to the river. To do this, the piezometers were previously grouped in the categories: maximum distance (i.e. piezometers farthest from the river banks: TOP2, TOP3, TOP4 and TOP10; between 140–460 m); medium distance (i.e. piezometers located at an intermediate distance from the river banks: TOP8 and TOP9; between 60–65 m) and minimum distance (i.e. piezometers closest to the river banks: TOP1, TOP5, TOP6 and TOP7; between 3–8 m). Finally, the relationships between bacterial communities (T-RFLP patterns data) and environmental parameters were determined by Canonical correspondence analysis (CCA) carried out using MVSP software (MultiVariate Statistical Package 3.12d, Kovach

Computing Services, 1985–2001, UK). Environmental parameters were scaled with the standardization transformation function of MVSP.

3. Results and discussion

3.1. Hydrological/hydrochemical characteristics and conceptual model

The record of hydraulic heads enabled groundwater flow patterns to be ascertained. In this regard, there is no hydraulic connection between the river and the alluvial aquifer, since the hydraulic heads of the river are systematically lower than those existing in the aquifer (Fig. 2). As a result, there is no recharge in the aquifer due to the occurrence of floods. In its stead, recharge is mainly produced by irrigation and, to a lesser extent, by precipitation.

As occurs in other riverine systems, concentrations of nitrates follow a spatio-temporal pattern, which is mainly determined by the application of fertilizers, both biological (i.e. pig slurry) and chemical, as well as by the irrigation practices that are put in practice (Arrate et al., 1997; Sánchez-Pérez et al., 2003b; Hernandez and Mitsch, 2007). Here, irrigation mainly takes place during the period between May and September. As a consequence, minimum concentrations of nitrates are given in August when irrigation is more intense and dilution processes more effective. In particular, in this month concentrations between 6.0 mg/L and 22.0 mg/L were measured. In contrast, November 2013 was when the highest concentrations of nitrates were measured, between 13 mg/L and 120.0 mg/L. These high concentrations may be a result of applying fertilizers and pig slurry (Diez et al., 2004). This pattern of spatio-temporal distribution also occurs with DOC. Therefore, minimum concentrations were recorded in August (1.5 mg/L), coinciding with the month in which irrigation is maximized. In contrast, November is when the COD concentrations were at a maximum (3.7 mg/L), due to the application of pig slurry to the soil.

As regards electrical conductivity, the measurements obtained were similar to those reported for the Ebro River (Spain) for the same sampling period (i.e. from April 2013 to March 2014; Antigüedad et al., in this issue). The study site may be divided into two sectors. The first, with a relatively significant load of pollutants, includes the piezometers named TOP5, TOP7, TOP8 and TOP9. In this sector, conductivities between 2193 and 3405 $\mu S\,cm^{-1}$ were measured during the period studied, whereas in the less polluted sector, which encompasses the piezometers TOP1, TOP2, TOP3, TOP4, TOP6 and TOP10, conductivities measured were between 955 and 2700 $\mu S\,cm^{-1}$. This difference seems to be related to how the agricultural practices explained above are implemented in the study site.

The data obtained enabled us to define a conceptual model based on consideration of the factors that determine dynamics at the study site (e.g. aquifer-river connectivity, groundwater dynamics, sources of pollution, etc.). In this regard, the most striking aspect was the absence of flood pulses (Junk et al., 1989). Thus, the soil did not present an adequate hydric status, and the carbon supply which provides energy to the bacteria directly responsible for the biogeochemical reactions that enable the elimination or reduction of pollutants (Fig. 3) was consequently reduced to the minimum.

3.2. Natural attenuation capacity

3.2.1. Enrichment/depletion of nitrates and DOC

The study site is not hydromorphologically functional, since there is no exchange of water between the river and the alluvial aquifer based on the existence of fluvial dynamics (Montoya et al., 2006). Therefore, the fact that the Tagus River is highly regulated causes the hydrograph to be static as far as flow variability is concerned. This hydrological regime is anomalous compared with other rivers in similar physiographic settings, e.g. the Ebro River, in Spain, or the Garonne River in France, where flood pulses in a given year alternate with low water flows (Antigüedad et al., in this issue).

With regard to the above, the main consequence of the absence of floods is the almost total loss of the riparian forest, which has mostly been replaced by agricultural land use and to a lesser extent by farms. Crops and farms currently occupy 87% of the meander, whereas the extension of the riparian forest is limited to only 13%. The result is soils with poor organic matter content compared to those developed in well-preserved wetlands. In addition, during the hydrological year it is very uncommon to find soils with high moisture and low oxygen content. The ideal conditions conducive to high denitrification rates are therefore not obtained in

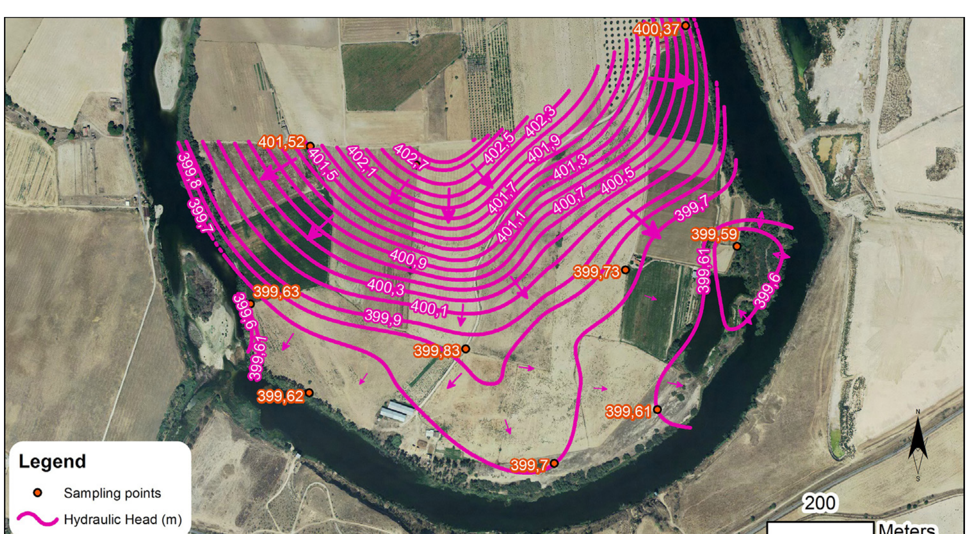

Fig. 2. Piezometric map showing groundwater flow directions and heads over the study area.

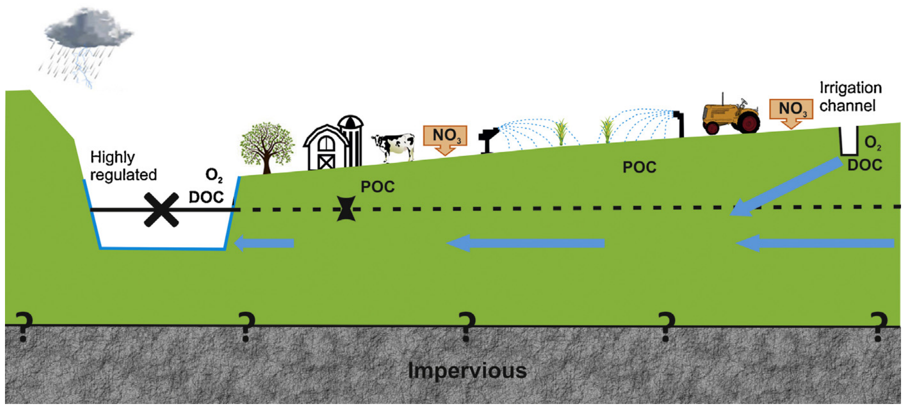

Fig. 3. Conceptual model of the study site.

the study site. However, the exchanges of water between the river and the aquifer are associated with the implementation of different irrigation practices that are generally highly inefficient, as the CTD diver records have shown (Fig. 4). As a result, specific zones of the study site receive large volumes of water coming from irrigation, thereby favoring dilution processes. In contrast, irrigation is less intense in the eastern part of the study site while the application of pig slurry is quite common; this explains why nitrates and COD present higher concentrations in this area. This scheme leads to a distinct water-mixing conceptual model for the study site. During the months where the irrigation water comes from this source there is a decrease toward the south, whereas water coming from the most polluted areas mainly decreases toward the west.

As a result of what is outlined above, two differentiated sectors may be recognized, in terms of the enrichment/depletion of nitrates and COD, and whose spatio-temporal variability is determined by agricultural management practices. Therefore, where irrigation is sufficiently high, negative variations of nitrates take place, which in this specific case means that depletion due to the existence of dilution processes may occur (Darwiche-Criado et al., 2015). In contrast, the eastern sector of the study site presents positive variations of nitrates during the whole period studied; this is a result of the agricultural practices explained previously. Regarding COD, a spatio-temporal pattern similar to the one described for the nitrates is observed (Fig. 5).

3.2.2. Macroinvertebrates as indicator of hydrologic connectivity

Compared with other lowland rivers of the Iberian Peninsula (e.g. Ebro river, see Gallardo et al., 2008), the diversity indices showed low variability (Fig. 6). 7 taxonomic groups (orders) were therefore identified in the piezometers. Crustaceans, particularly Ostracods, was the most important taxonomic group, representing 62.6% of the total invertebrates abundance (ranging from 72 to 221) individuals per 100 L water pumped; $n = 529$) followed by stenasellid Isopods (10.8%; $n = 92$), Nematods (3.4%; $n = 24$), cyclopoid Copepods (2.3%; $n = 20$), Oligochaeta (2.3%; $n = 20$) and others (18.2%; $n = 150$), including in this last category Amphipods (1.4%; $n = 7$) and Branchiopods (0.6%; $n = 5$). The fact that Ostracoda is the most abundant taxon, is often associated with low groundwater level fluctuations (Malard et al., 1996), in accordance with the low river discharge fluctuations recorded in the study site during the study period (5–7 $m^3\ seg^{-1}$). The dominant functional group was deposit-feeders (76%), followed by filter-feeders (12%), scrappers (5%), shredders (3%), predators (2%), piercers (1%) and absorbers (1%).

From a temporal point of view, the diversity indices considered did not show statistically significant differences between the four quarterly sampling campaigns (i.e. in all cases P-values were higher than 0.05). In contrast, at the spatial level statistically significant differences were found. With regard to this, total abundance and taxonomic richness were significantly higher (P-values less than

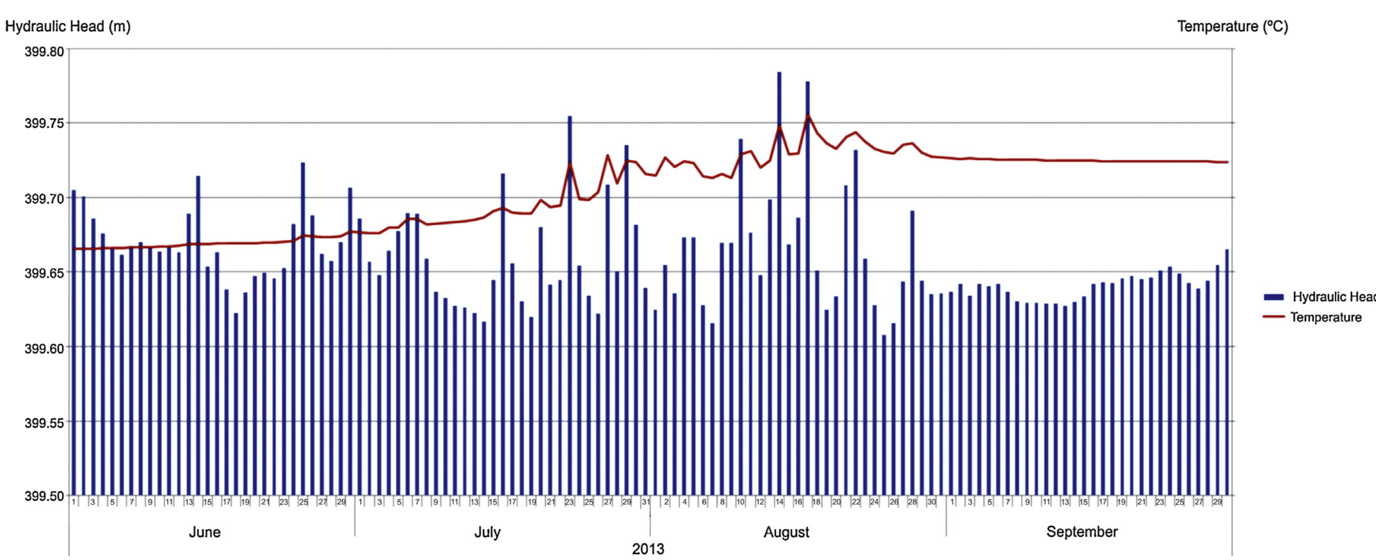

Fig. 4. The arrival of irrigation water to the groundwater was detected by the CTD divers by synchronous increments of temperature (red line) and hydraulic heads (blue bars). (For interpretation of the references to colour in this figure legend, the reader is referred to the web version of this article.)

Please cite this article in press as: Bodoque, J.M., et al., Recovering hydromorphological functionality to improve natural purification capacity of a highly human-modified wetland. Ecol. Eng. (2016), http://dx.doi.org/10.1016/j.ecoleng.2016.02.013

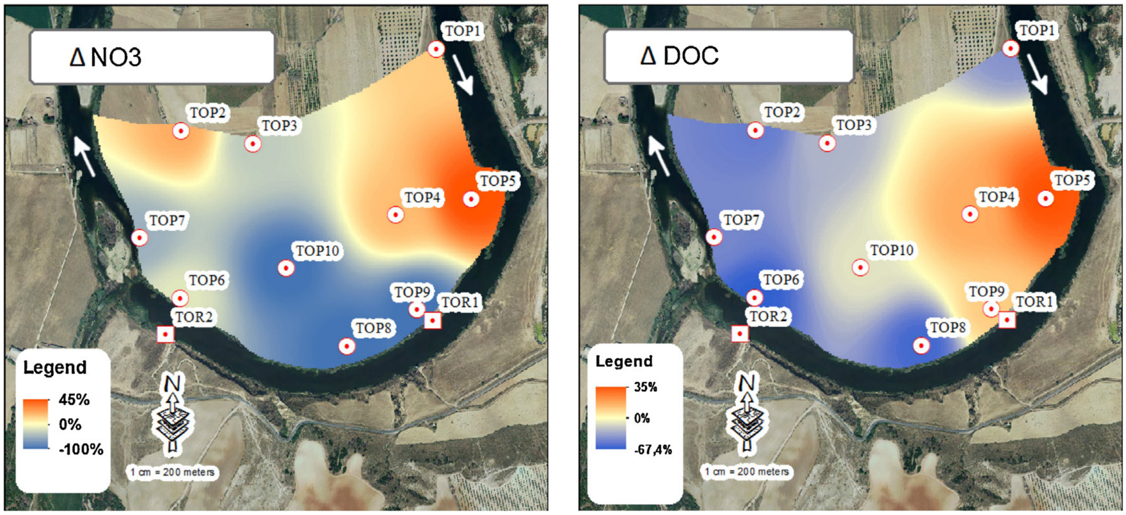

Fig. 5. Spatial distribution of the rate of NO_3^- (ΔNO_3^-) and DOC (ΔDOC) calculated by the two poles mixing model.

0.01) in piezometers TOP1, TOP5, TOP6 and TOP7. A similar pattern was detected in the distribution of Shannon diversity and taxonomic evenness, though for these indices the differences found were not statistically significant (*P*-values higher than 0.05; Fig. 7). The dissimilarity described above is a result of the proximity of the piezometers to the river. The piezometers closest to the river banks showed the highest diversity, whereas those farthest away had the lowest diversity. The piezometers TOP8 and TOP9, located at an intermediate distance from the river banks, showed a higher diversity than the group of piezometers situated farther from the river, and lower than the diversity estimated for the piezometers that were closer to it. These results match those obtained by other authors, who reported an increase in invertebrate richness with hydrological connectivity (e.g. Ward et al., 2002; Gallardo et al., 2008). In the specific case of the Tagus River, its high level of regulation has minimized the occurrence of floods and, therefore, connectivity between water bodies is virtually nonexistent. Consequently, the mobility of invertebrates along with the interchange of water, nutrients and organic matter between the river and the floodplain has been drastically reduced, which has very negative consequences for river ecosystem biodiversity, function and processes (Amoros and Roux, 1988).

3.2.3. Denitrification potential

Two sectors from the point of view of potential denitrification can be recognized in the study area (Fig. 8). The first (S1 sector) encompasses the piezometers TOP5, TOP7, TOP8 and TOP9, whilst the second (S2 sector) includes the piezometers TOP1,

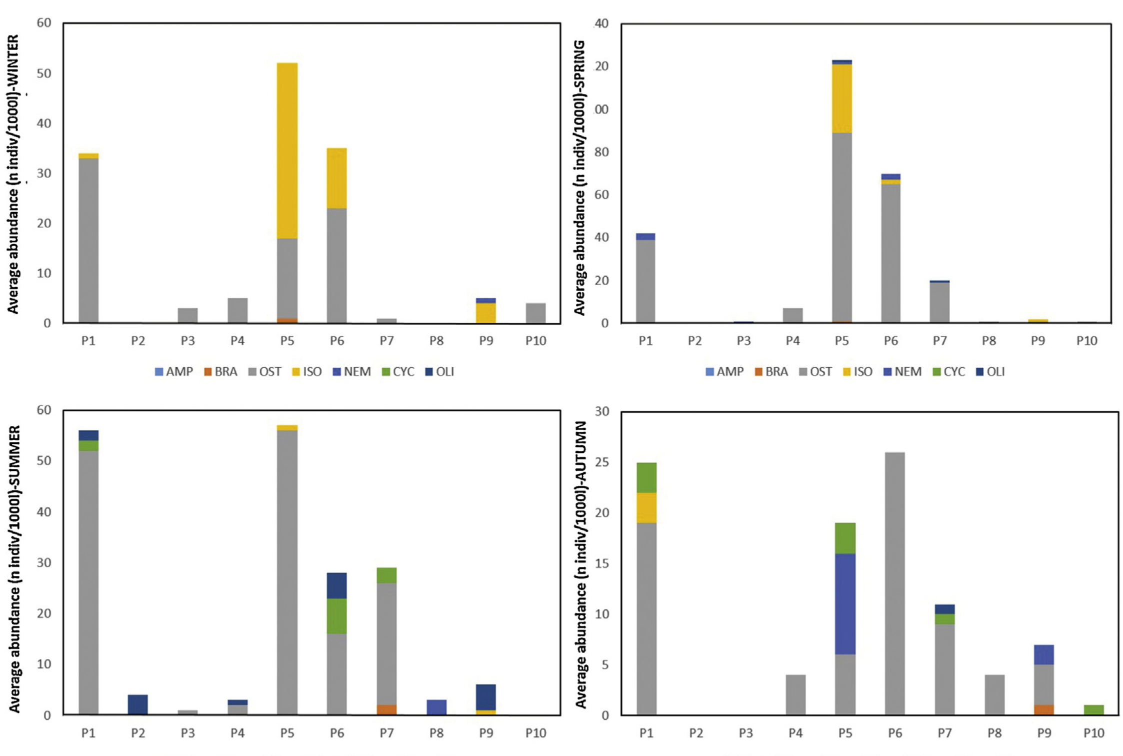

Fig. 6. Macroinvertebrate taxonomic diversity metrics. Data are mean values of each of the quarterly sampling campaigns conducted between April 2013 and February 2014 (AMP = Amphipoda; BRA = Branchiopoda; OST = Ostracoda; ISO = Isopoda Stenasellidae; NEM = Nematoda; CYC = Copepoda Cyclopoida; OLI = Oligochaeta; HET = Heteroptera).

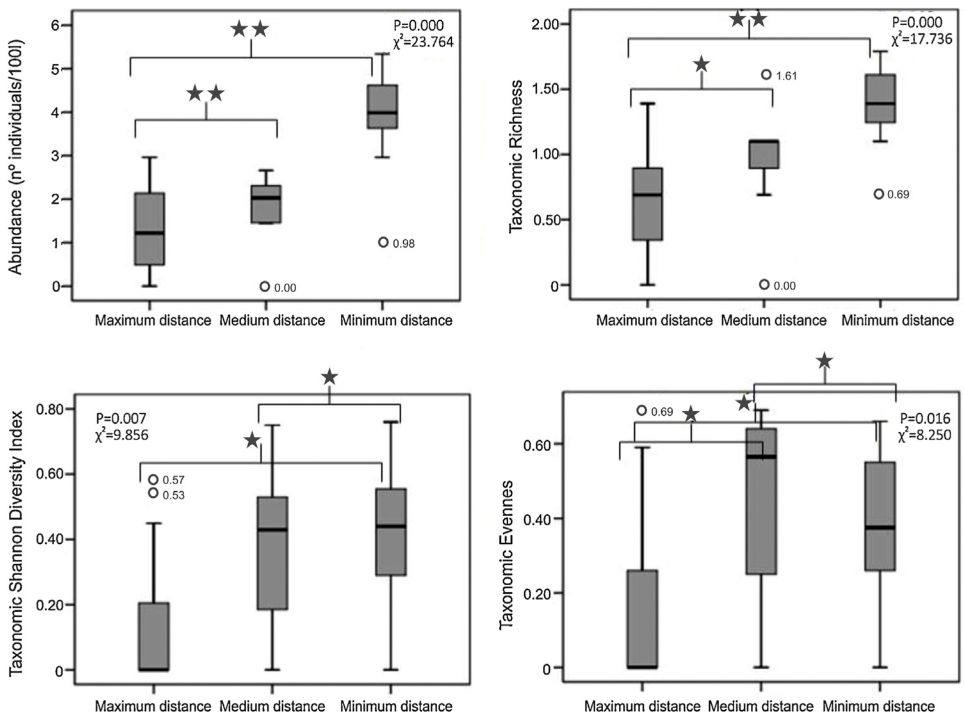

Fig. 7. Taxonomic diversity depending on the distance from the river banks. Results from non-parametric analysis of variance (Kruskal–Wallis method) between the categories: minimum distance; medium distance and maximum distance. Spatial variability over the year corresponding with *F* values (ANOVA) and chi-square values (Kruskal–Wallis) and significance level are given on the top right corner of this figure. Significant levels between categories are indicated with $^{*}P<0.05$ and $^{**}P<0.01$. *Circles* and *asterisks* show outliers.

TOP2, TOP3, TOP4, TOP6 and TOP10. In S1, denitrification potential rates were between 6.2 and 390.0 μg N-N_2O h^{-1} g^{-1} MO, with 92.6 μg N-N_2O h^{-1} g^{-1} MO being the average value. In S2 rates were between 1.7and 152.8 μg N-N_2O h^{-1} g^{-1} and had an average value of 18.8 μg N-N_2O h^{-1} g^{-1} MO. The highest denitrification potential rates have been estimated in S1 and is a result of some of the most favorable local conditions obtained in this sector, especially as far as the concentration of nitrates and dissolved oxygen is concerned (Venterink et al., 2003). In S1 the average measured concentration of nitrates was 46.1 mg/L, while in S2 it was 31.9 mg/L. S1 showed the lowest oxygen values (i.e. 13.7% on average), while values in S2 were higher. Specifically, an average concentration of 50.8% was estimated.

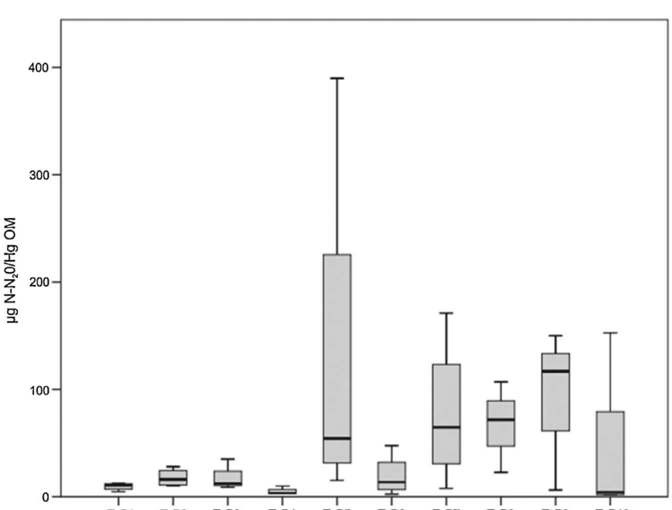

Fig. 8. Box and whisker plot showing average denitrification potential in each piezometer.

The multiple analysis correlation (Table 1) shows the existence of significant statistical correlation between denitrification potential and redox potential ($r=-0.398$, $P<0.05$), which coincides with the results obtained by other authors (Brettar et al., 2002). Therefore, the piezometers included in S1 that, on the other hand, had the highest denitrification rates, recorded values of potential redox between −154 mV and 155.6 mV, while in S2 (where the lowest denitrification rates were estimated) redox potential was between −37.7 mV and 203.0 mV. A significant statistical correlation was also found with nitrate concentration ($r=0.361$, $P<0.05$), which makes sense as the presence of nitrates is one of the factors needed to make denitrification possible (Martin et al., 1999).

With the exception of sampling campaign 1, all of the campaigns had similar average denitrification values (Fig. 9). In this regard, the Kruskal–Wallis ANOVA showed significant statistical differences (*P*-values less than 0.05) in mean denitrification values between the first campaign (April 2013) and the other quarterly campaigns ($\chi^2=9.29$, df = 3, $P=0.026$). However, significant statistical differences were not detected between campaigns 2, 3 and 4 (i.e. July 2013, October 2013 and January 2014). This behavior is contrary to what usually occurs in areas that are biogeochemically functional. In this context, DEA measurements indicate strong spatio-temporal heterogeneity, which is a result of the occurrence of flood pulses (Bernard-Jannin et al., 2015).

A comparison of the piezometers shows that TOP5, TOP7, TOP8 and TOP9 are statistically different when compared with piezometers P1, P2, P3, P4 and P10 ($\chi^2=11.89$, df = 1, $P=0.001$). However, these differences are not related to flood pulses, as shown by the piezometric maps (see Fig. 2). In addition, these results show that irrigation does not seem to cause denitrification potential rates that are significantly higher than those estimated during the period of the year with no irrigation. The differences found are a result of the dissimilar load of pollution concerning nitrates detected between the two groups of piezometers. An explanation for the differences between campaigns is not so obvious, though it might be related

Please cite this article in press as: Bodoque, J.M., et al., Recovering hydromorphological functionality to improve natural purification capacity of a highly human-modified wetland. Ecol. Eng. (2016), http://dx.doi.org/10.1016/j.ecoleng.2016.02.013

Table 1
Spearman's rho correlation between denitrification potential and main physico-chemical parameters.

		O2 (%)	pH	EC (μS cm^{-1})	ORP (mV)	DOC (mg/L)	NO_3 (mg/L)	μg N-N_2O h^{-1} g^{-1} MO
	Correlation coefficient	1	**0.778****	**−0.791****	−0.245	0.260	−0.425*	−0.071
O_2 (%)	Sig. (2-tailed)		**0.000**	**0.000**	0.177	0.150	0.015	0.708
	n	32	**32**	**32**	32	32	32	30
	Correlation coefficient	**0.778****	1	**−0.765****	0.028	**0.368***	−0.243	0.026
pH	Sig. (2-tailed)	**0.000**		**0.000**	0.860	**0.038**	0.180	0.875
	N	**32**	42	**42**	42	**32**	32	39
	Correlation coefficient	**−0.791****	**−0.765****	1	0.194	−0.149	0.247	−0.118
EC (μS cm^{-1})	Sig. (2-tailed)	**0.000**	**0.000**		0.219	0.415	0.173	0.476
	N	**32**	**42**	42	42	32	32	39
	Correlation coefficient	−0.245	0.028	0.194	1	0.339	0.238	**−0.398***
ORP (mV)	Sig. (2-tailed)	0.177	0.860	0.219		0.058	0.189	**0.012**
	N	32	42	42	42	32	32	**39**
	Correlation coefficient	0.260	**0.368***	−0.149	0.339	1	0.067	0.303
DOC (mg/L)	Sig. (2-tailed)	0.150	**0.038**	0.415	0.058		0.709	0.097
	N	32	**32**	32	32	33	33	31
	Correlation coefficient	**−0.425***	−0.243	0.247	0.238	0.067	1	**0.361***
NO_3 (mg/L)	Sig. (2-tailed)	**0.015**	0.180	0.173	0.189	0.709		**0.046**
	N	**32**	32	32	32	33	33	**31**
	Correlation coefficient	−0.071	0.026	−0.118	**−0.398***	0.303	**0.361***	1
μg N-N_2O h^{-1} g^{-1} MO	Sig. (2-tailed)	0.708	0.875	0.476	**0.012**	0.097	**0.046**	
	N	30	39	39	**39**	31	**31**	40

* Significant level between categories are indicated with $P < 0.05$.
** Significant level between categories are indicated with $P < 0.01$.

to the fact that during the months immediately before April 2013 the alluvial aquifer was not recharged with water coming from irrigation. The above could explain negative potential redox in several piezometers as well as the low oxygen measured.

3.2.4. Bacterial assemblage structures and possible implications concerning attenuation

The bacterial assemblage structures were determined by T-RFLP based on 16S rRNA genes analysis. The T-RFLP patterns showed between 4 and 25 T-RFs (terminal restriction fragments; or OTUs, operational taxonomic units) with an average of 14.4 ± 4.1 T-RFs. Similar OTU-richness has been reported in hyporheic zones of an intermittent stream before flooding (Febria et al., 2012). The Shannon index ranged from 1.4 to 3.1 (average 2.3 ± 0.3) and Evenness ranged from 0.69 to 0.99 (average 0.9 ± 0.05).

In order to reveal the factors related with bacterial communities structures, the relationships between bacterial populations (T-RFLP OTUs) and environmental parameters were determined by canonical correspondence analyses (CCA) correlating T-RFLP patterns with the chemical contents (Fig. 10). Most bacterial communities were grouped indicating that the bacterial communities structures were similar irrespective of the location and the sampling date (Fig. 10a) as previously shown in the hyporheic zone of

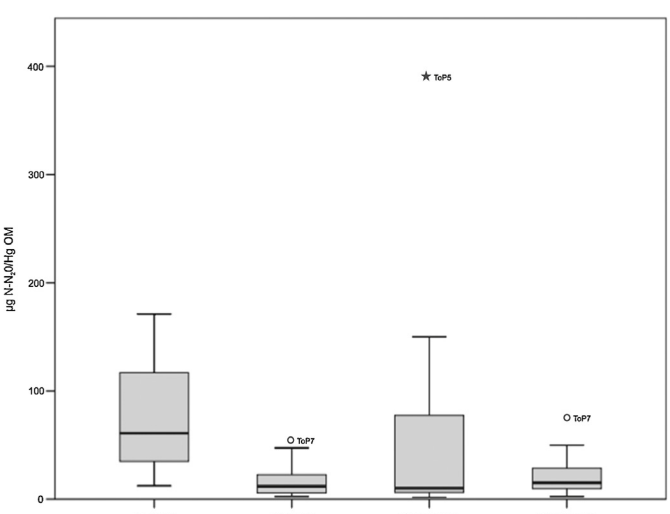

Fig. 9. Box and whisker plot showing average denitrification potential for each quarterly sampling campaign. *Circle* and *asterisk* represent outliers.

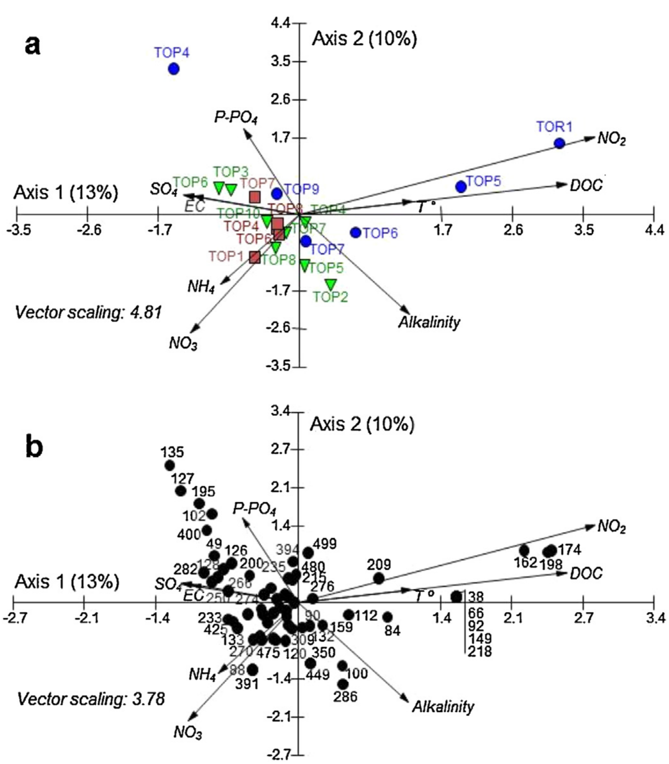

Fig. 10. Canonical correspondence analysis (CCA) correlating (A) bacterial communities (T-RFLP patterns) and (B) bacterial populations (T-RFLP OTUs) with environmental parameters (nitrogen forms: NO_2, NO_3 and NH_4; DOC: dissolved organic carbon; T°: temperature; alkalinity; sulfate: SO_4; phosphate: P-PO_4; EC: electrical conductivity). The analysis is based on 16S rRNA gene T-RFLP profiles from sediments collected in February (blue circles), July (green triangles) and October (brown squares). (For interpretation of the references to colour in this figure legend, the reader is referred to the web version of this article.)

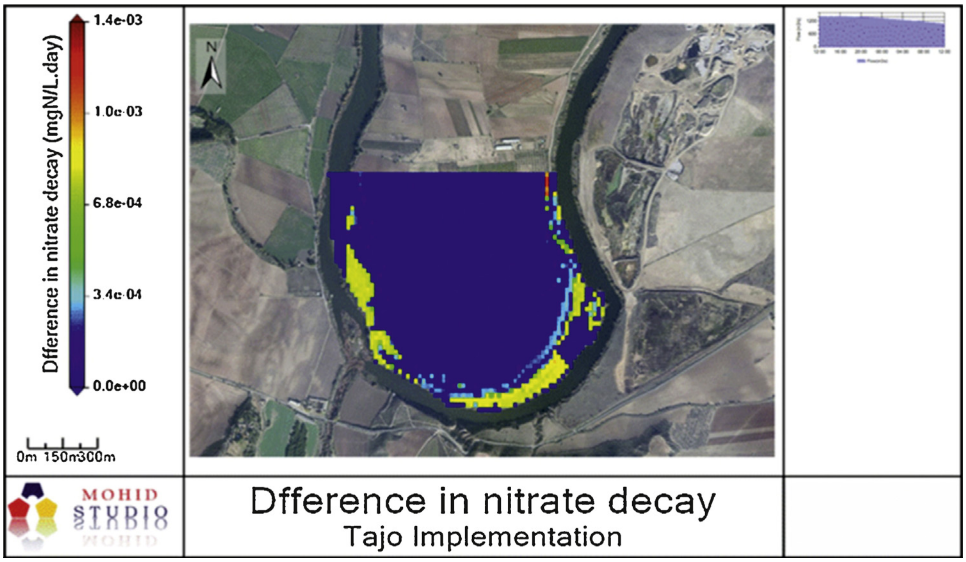

Fig. 11. Difference in nitrate decay in alluvial aquifer considering the scenario in which the Tagus River would experiment floods.

an intermittent stream (Febria et al., 2012). The CCA, explaining 23% of the data distribution, showed that the bacterial communities in the TOP5 station in February were distributed along the axis 1 (13% of the distribution) and were mostly associated to DOC and NO_2, which may be related to the existence of partial denitrification (Fig. 10a). For the same sampling date, in the TOP4 station the bacterial assemblage structure was linked with phosphate (P-PO_4). In contrast, bacterial communities in July and October were distributed along the axis 2 (10% of the distribution). The bacterial communities of TOP2 and TOP5 stations were associated to alkalinity in July while those of TOP1, TOP4 and TOP6 stations were correlated to NH_4 and NO_3 in October (Fig. 10a), suggesting a coupled nitrification–denitrification as previously demonstrated in high nitrate containing stream (Smith et al., 2009). However, most bacterial communities are not linked with NH_4 or NO_3, which probably indicates that for practical purposes denitrification activity is of little importance.

The CCA also revealed some specific OTUs correlated to environmental parameters that explained the differences observed between the stations (Fig. 10b). Four OTUs (102, 127, 135 and 195) were associated with phosphate; they determine the specificity of the bacterial assemblage of the TOP4 station in July. Previous studies have demonstrated the influence of phosphate on bacterial communities in soil (Kuramae et al., 2012) and hyporheic zones (Febria et al., 2012). Three OTUs (162, 174 and 198) were strongly correlated with NO_2 and DOC suggesting that these OTUs may be related to ammonia oxidizing bacteria (AOB), first step of the nitrification process. The correlation between AOB and DOC has been observed in groundwater (van der Wielen et al., 2009). It is likely that these OTUs participate to the depuration of the system during winter season at station TOP4. In contrast, two OTUs (88 and 391) were associated with nitrate and ammonium; they may correspond either to bacteria involved in nitrification or denitrification processes.

3.2.5. Hydrological modeling

What differentiates the Tagus from most other rivers in its class (e.g. Ebro River in Spain, or Garonne River in France) is its poor hydromorphological quality in most of its reaches (Antigüedad et al., in this issue). As a result, the river has hardly any capacity to recharge the alluvial aquifer, unless recharge is artificially induced through irrigation, as occurs in the study site. In this context, the model was able to represent the increase in level due to irrigation water. Concerning nitrate aquifer concentrations, acceptable results are also obtained when comparing model results and field data aquifer concentrations for around 1 month and 2 months after the model start. Since the site is not flooded, water quality processes take a long time to occur, and the decay change is very stable, on the order of 0.01 mg N/L day (1 mg N decay in 3 months).

Since the Tagus River is characterized by very low hydrodynamics, and nitrate concentrations do not limit the processes of depuration, almost none of the scenarios studied implied any significant improvement in water quality. Only one scenario, in which the Tagus had floods with a peak of 1400 $m^3\,s^{-1}$, yielded favorable results in this regard. This result is shown in Fig. 11, where nitrate decay differences compared to the reference scenario are presented. It can be seen that in the areas near the river (which are flooded) nitrate decay increases (around 10%). So, it is a well-known fact that fluctuating surface water levels due to floods create particularly effective conditions for enhancing denitrification, since they determines oxygen-limited conditions and carbon supply (Forshay and Stanley, 2005).

This condition hardly exists in the Tagus River since its hydromorphological conditions deviate greatly from the unaltered conditions as a result of its hydrological regime. The Tagus watershed has 283 reservoirs and 40 diversion channels, including the Tagus–Segura inter-basin water transfer system, which transfers an average annual volume of 350 Hm^3 to the Segura basin (located in south-eastern Spain). As a result, having significantly decreased the frequency of what yesteryear were ordinary floods, agriculture has expanded almost to the point of causing the disappearance of the riparian forest, which have affected site functionality and natural depuration processes. Nevertheless, the results derived from the model show that the hydromorphological and ecological functionality of the Tagus River can be partially recovered if riverine wetlands are restored while favoring the occurrence of flood pulsing.

4. Conclusions

The methodological approach implemented shows that natural purification is almost nonexistent at the study site. This is due to how highly regulated the Tagus River is, which determines that for practical purposes surface water levels remain stable. As a result, the floodplain is no longer flooded and agriculture has occupied most of the former riparian wetland. Under these circumstances, the environmental factors needed to activate the biogeochemical process of water quality improvement do not exist. In addition, the equally necessary organic carbon supply has been significantly reduced due to the almost total disappearance of the riparian forest. The above was also corroborated by both an analysis of bacterial assemblage structure and macroinvertebrates, which demonstrated that denitrification activity is practically nonexistent. Modeling of the scenarios showed that in order to restore natural groundwater purification, it will be crucial to improve hydromorphology by achieving a less altered hydrological regime that favors the occurrence of flood pulses.

Acknowledgements

This study was conducted as part of the EU Interreg SUDOE IVB programme (ATTENAGUA – SOE3/P2/F558 project, http://www.attenagua-sudoe.eu) and was funded by the European Regional Development Fund (ERDF).

References

Amoros, C., Roux, A.L., 1988. Interaction between water bodies within the floodplain of large rivers: function and development of connectivity. Münstersche Geogr. Arb. 29, 125–130.

Antigüedad, I., Zabaleta, A., Martinez-Santos, M., Ruiz-Romera, E., Uriarte, J., Morales, T., Francisco, A., Comin, F.A., Carranza, F., Español, C., Navarro, E., Bodoque, J.M., Ladera, J., Brito, D., Neves, R., Bernard-Jannin, L., Sun, X., Teissier, S., Sauvage, S., Sanchez-Perez, J.M. From hydrochemical observation to hydrological conceptualization: a multi-criteria assessment in four different riparian zones. Ecol. Eng. (in this issue).

Arrate, I., Sánchez-Pérez, J.M., Antigüedad, I., Vallecillo, M.A., Iribar, V., Ruiz, M., 1997. Groundwater pollution in quaternary aquifer of Vitoria: Gasteiz (Basque Country, Spain): influence of agricultural activities and water-resource management. Environ. Geol. 30, 257–265.

Bernard-Jannin, L., Sun, X., Teissier, S., Sauvage, S., Sánchez-Pérez, J.M., 2015. Spatio-temporal analysis of potential denitrification hot spots and hot moments in groundwater and their impact on nitrate dynamics in an alluvial floodplain. Ecol. Eng., http://dx.doi.org/10.1016/j.ecoleng.2015.12.031.

Boulton, A.J., Fenwick, G.D., Hancock, P.J., Harvey, M.S., 2008. Biodiversity, functional roles and ecosystem services of groundwater invertebrates. Invertebr. Syst. 22, 103–116.

Brettar, I., Sánchez-Perez, J.M., Tremolieres, M., 2002. Nitrate elimination by denitrification in hardwood forest soils of the Upper Rhine floodplain – correlation with redox potential and organic matter. Hydrobiologia 469 (1–3), 11–21.

Christophersen, N., Neal, C., Hooper, R.P., Vogt, R.D., Andersen, S., 1990. Modeling streamwater chemistry as a mixture of soilwater end-members – a step towards 2nd generation acidification models. J. Hydrol. 116 (1–4), 307–320.

Culman, S.W., Bukowski, R., Gauch, H.G., Cadillo-Quiroz, H., Buckley, D.H., 2009. T-REX: software for the processing and analysis of T-RFLP data. BMC Bioinform. 10, 171.

Darwiche-Criado, N., Comin, F.A., Sorando, R., Sánchez-Pérez, J.M., 2015. Seasonal variability of NO_3 – mobilization during flood events in a Mediterranean catchment: the influence of intensive agricultural irrigation. Agric. Ecosyst. Environ. 200, 208–218.

Diez, J.A., Hernaiz, P., Munoz, M.J., de la Torre, A., Vallejo, A., 2004. Impact of pig slurry on soil properties, water salinization, nitrate leaching and crop yield in a four-year experiment in Central Spain. Soil Use Manag. 20 (4), 444–450.

European Commission, Brussels, Belgium 2000. Directive 2000/60/EC of the European Parliament and of the Council of 23 October 2000 Establishing a Framework for Community Action in the Field of Water Policy. Official Journal L 327, 22/12/2000., pp. 73.

Febria, C.M., Beddoes, P., Fulthorpe, R.R., Williams, D.D., 2012. Bacterial community dynamics in the hyporheic zone of an intermittent stream. ISME J. 6, 1078–1088.

Forshay, K.J., Stanley, E.H., 2005. Rapid nitrate loss and denitrification in a temperate river floodplain. Biogeochemistry 75 (1), 43–64.

Gallardo, B., García, M., González, E., González, M., Ciancarelli, C., Comín, F.A., 2008. Macroinvertebrate patterns along environmental gradients and hydrological connectivity within a regulated river-floodplain. Aquat. Sci. 70 (3), 248–258.

Groffman, P.M., Butterbach-Bahl, K., Fulweiler, R.W., Gold, A.J., Morse, J.L., Stander, E.K., Tague, C., Tonitto, C., Vidon, P., 2009. Challenges to incorporating spatially and temporally explicit phenomena (hotspots and hot moments) in denitrification models. Biogeochemistry 93 (1–2), 49–77.

Hernandez, M.E., Mitsch, W.J., 2006. Influence of hydrologic pulses, flooding frequency, and vegetation on nitrous oxide emissions from created riparian marshes. Wetlands 26 (3), 862–877.

Hernandez, M.E., Mitsch, W.J., 2007. Denitrification in created riverine wetlands: influence of hydrology and season. Ecol. Eng. 30 (1), 78–88.

Hunt, P.G., Miller, J.O., Ducey, T.F., Lang, M.W., Szogi, A.A., McCarty, G., 2014. Denitrification in soils of hydrologically restored wetlands relative to natural and converted wetlands in the Mid-Atlantic coastal plain of the USA. Ecol. Eng. 71, 438–447.

Iribar, A., Sánchez-Pérez, J.M., Lyautey, E., Garabétian, F., 2008. Differentiated free-living and sediment-attached bacterial community structure inside and outside denitrification hotspots in the river–groundwater interface. Hydrobiologia 598, 109–121.

Junk, W.J., Bayley, P.B., Sparks, R.E., 1989. The flood pulse concept in river-floodplain systems. Can. Spec. Publ. Fish. Aquat. Sci. 106, 110–127.

Kingsford, R.T., 2000. Ecological impacts of dams, water diversions and river management on floodplain wetlands in Australia. Austral Ecol. 25 (2), 109–127.

Kjellin, J., Hallin, S., Worman, A., 2007. Spatial variations in denitrification activity in wetland sediments explained by hydrology and denitrifying community structure. Water Res. 41 (20), 4710–4720.

Kuramae, E.E., Yergeau, E., Wong, L.C., Pijl, A.S., van Veen, J.A., Kowalchuk, G.A., 2012. Soil characteristics more strongly influence soil bacterial communities than land-use type. FEMS Microbiol. Ecol. 79, 12–24.

Lane, D.J., 1991. 16S/23S rRNA sequencing. In: Stachenbrady, E., Goodfellow, M. (Eds.), Nucleic Acid Techniques in Bacterial Systematics. John Wiley & Sons, New York, NY, pp. 115–175.

Martin, T.L., Kaushik, N.K., Trevors, J.T., Whiteley, H.R., 1999. Review: denitrification in temperate climate riparian zones. Water Air Soil Pollut. 111 (1–4), 171–186.

Malard, F., Mathieu, J., Reygrobellet, J.-L., Lafont, M., 1996. Biomotoring groundwater contamination: application to a karst area in Southern France. Aquat. Sci. 58, 158–187.

Mermillod-Blondin, F., Gaudet, J.P., Gerino, M., Desrosiers, G., des Chatelliers, M.C., 2003. Influence of macroinvertebrates on physico-chemical and microbial processes in hyporheic sediments. Hydrol. Process. 17 (4), 779–794.

Middleton, B.A., 2002. The flood pulse concept in wetland restoration. In: Middleton, B.A. (Ed.), Flood Pulsing in Wetlands: Restoring the Natural Hydrological Balance. John Wiley & Sons, Inc., New York, USA, pp. 1–10.

Montoya, F.J.F., del Pozo, G.L., de Andres, M.A.O., Colmenar, J.M., 2006. Consequences of the regulating dams at the head of the Tagus River in the management of water supply, hydropower and flood prevention. In: International Symposium on Dams in the Societies of the 21st Century. Proceedings and Monographs in Engineering, Water and Earth Sciences, Barcelona, Spain, pp. 113–116.

Peyrard, D., Delmotte, S., Sauvage, S., Namour, P., Gerino, M., Vervier, P., Sánchez-Pérez, J.M., 2011. Longitudinal transformation of nitrogen and carbon in the hyporheic zone of an N-rich stream: a combined modelling and field study. Phys. Chem. Earth 36 (12), 599–611.

Pinay, G., Clement, J.C., Naiman, R.J., 2002. Basic principles and ecological consequences of changing water regimes on nitrogen cycling in fluvial systems. Environ. Manag. 30 (4), 481–491.

Rabot, E., Henault, C., Cousin, I., 2014. Temporal variability of nitrous oxide emissions by soils as affected by hydric history. Soil Sci. Soc. Am. J. 78 (2), 434–444.

Sánchez-Pérez, J.M., Trémolières, M., 2003. Change in groundwater chemistry as a consequence of suppression of floods: the case of the Rhine floodplain. J. Hydrol. 270, 89–104.

Sánchez-Pérez, J.M., Vervier, P., Garabetian, F., Sauvage, S., Loubet, M., Rols, J.L., Bariac, T., Weng, P., 2003a. Nitrogen dynamics in the shallow groundwater of a riparian wetland zone of the Garonne, SW France: nitrate inputs, bacterial densities, organic matter supply and denitrification measurements. Hydrol. Earth Syst. Sci. 7 (1), 97–107.

Sánchez-Pérez, J.M., Antigüedad, I., Arrate, I., García-Linares, C., Morell, I., 2003b. The influence of nitrate leaching through unsaturated soil on groundwater pollution in an agricultural area of the Basque country: a case study. Sci. Total Environ. 317, 173–187.

Smith, M.S., Tiedje, J.M., 1979. Phases of denitrification following oxygen depletion in soil. Soil Biol. Biochem. 11 (3), 261–267.

Smith, R.L., Böhlke, J.K., Repert, D.A., Hart, C.P., 2009. Nitrification and denitrification in a midwestern stream containing high nitrate: in situ assessment using tracers in dome-shaped incubation chambers. Biogeochemistry 96, 189–208.

Song, K., Hernandez, M.E., Batson, J.A., Mitsch, W.J., 2014. Long-term denitrification rates in created riverine wetlands and their relationship with environmental factors. Ecol. Eng. 72, 40–46.

Tachet, H., Richoux, P., Bournaud, M., Usseglio-Polatera, P., 2010. Invertébrés d'eau douce. Systématique, biologie, écologie. CNRS Editions, Paris, pp. 607.

Teske, A., Wawer, C., Muyzer, G., Ramsing, N.B., 1996. Distribution of sulfate-reducing bacteria in a stratified fjord (Mariager Fjord, Denmark) as evaluated by most-probable-number counts and denaturing gradient gel electrophoresis of PCR-amplified ribosomal DNA fragments. Appl. Environ. Microbiol. 62, 1405–1415.

Trancoso, A.R., Braunschweig, F., Leitao, P.C., Obermann, M., Neves, R., 2009. An advanced modelling tool for simulating complex river systems. Sci. Total Environ. 407 (8), 3004–3016.

van der Wielen, P.W.J.J., Voost, S., van der Kooij, D., 2009. Ammonia-oxidizing bacteria and archaea in groundwater treatment and drinking water distribution systems. Appl. Environ. Microbiol. 75, 4687–4695.

Venterink, H.O., Hummelink, E., Van den Hoorn, M.W., 2003. Denitrification potential of a river floodplain during flooding with nitrate-rich water: grasslands versus reedbeds. Biogeochemistry 65 (2), 233–244.

Volant, A., Bruneel, O., Desoeuvre, A., Héry, M., Casiot, C., Bru, N., Delpoux, S., Fahy, A., Javerliat, F., Bouchez, O., Duran, R., Bertin, P.N., Elbaz-Poulichet, F., Lauga, B., 2014. Diversity and spatiotemporal dynamics of bacterial communities: physicochemical and other drivers along an acid mine drainage. FEMS Microbiol. Ecol. 90, 247–263.

Ward, J.V., Tockner, K., Arscott, D.B., Claret, C., 2002. Riverine landscape diversity. Freshw. Biol. 47 (4), 517–539.